ACS OMEGA

http://pubs.acs.org/journal/acsodf

Article

Methylenedisalicylic Acid as a Biocorrosion Inhibitor for Aluminum in Concentrated Sodium Chloride Solutions

Ayman H. Ahmed* and El-Sayed M. Sherif

Cite This: *ACS Omega* 2022, 7, 19193−19203

Read Online

ACCESS | Metrics & More | Article Recommendations

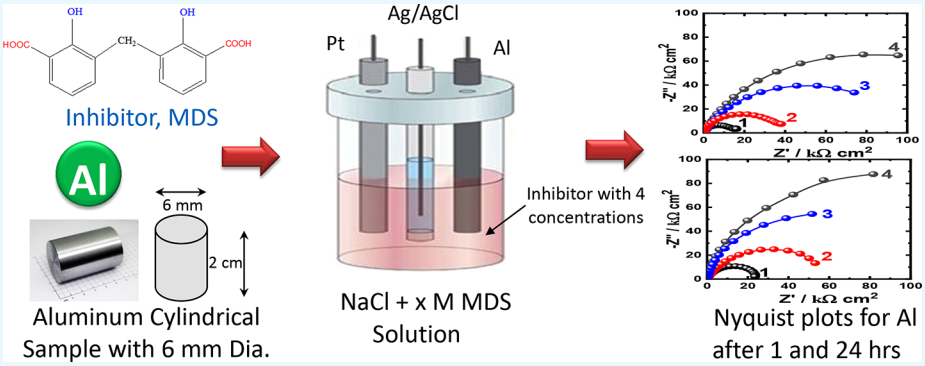

ABSTRACT: 3,3′-Methylenedisalicylic acid (MDS) was synthesized and ascertained on the basis of elemental analyses (C, H) and spectral measurements (IR, mass, ^{1}H NMR, and UV−vis). Moreover, the prepared MDS compound has been assayed for its antimicrobial action against the growth of fungi as well as Gram-positive and Gram-negative bacteria. The results demonstrated the possibility of its usefulness to restrain the growth of both fungi and bacteria, whereas MDS showed its best impact against *Candida albicans*. The inhibitive impact of MDS on the corrosion of aluminum (Al) in concentrated sodium chloride solution (3.5 wt % NaCl) has been investigated. The corrosion work was done by potentiodynamic cyclic polarization, electrochemical impedance spectroscopy, and chronoamperometric current−time measurements and complemented by scanning electron microscopy and energy-dispersive X-ray investigations. It was found that MDS molecules protect the aluminum against corrosion, and its ability increases with the increase of concentration from 5×10^{-5} to 1×10^{-4} M and further to 5×10^{-4} M. The electrochemical results were supported by the morphological analysis and proved that the presence of MDS inhibits the uniform and pitting corrosion of Al in the chloride solutions.

1. INTRODUCTION

Aluminum is the third most predominant element and the most abundant metal in the earth's crust, representing about 8% of total mineral components. The main important features of aluminum are its low density and nontoxicity. The high thermal and electrical conductivity of aluminum, in addition to its relatively low price, makes it useful in various applications.[1] In modern society, aluminum has common and valuable applications in electrical lines, window frames, high-rise buildings, consumer electronics, aircraft components, industrial and household appliances, spacecraft components, trains, ships, and personal vehicles. In terms of corrosion, aluminum by itself is not resistant; however, if an oxide layer is formed on the surface, it becomes highly resistant to corrosive attack in various media. However, when exposed to chloride, alkaline and acid-containing media, the oxide layer is damaged, causing the aluminum to be susceptible to the corrosive environment.[2,3] Different techniques can be utilized to protect aluminum and its alloys. It is convenient to employ corrosion inhibitors. Most of the well-known inhibitors are organic compounds containing π bonds, O, P, N, and S, as well as aromatic rings in their composition, which are the significant adsorption centers.[4]

According to the literature, numerous organic and inorganic compounds are used as inhibitors in controlling corrosion of aluminum in chloride media. Among these inorganic inhibitors, cerium(III) acetate and Ce(III, IV) ammonium nitrate have been employed as corrosion inhibitors for AA2024 aluminum alloys.[5,6] With regard to preservation of aluminum in 3.5% NaCl solution using organic inhibitors, some

Received: January 10, 2022
Accepted: March 11, 2022
Published: June 1, 2022

substances have been assessed. Sherif and Park assessed the inhibition impact of 1,4-naphthoquinone (NQ) as a corrosion inhibitor for aluminum in 0.5 M NaCl solutions using various electrochemical techniques [potentiodynamic polarization (PDP) and electrochemical impedance spectroscopy (EIS)].[7] The restraint effectiveness in both aerated and deaerated solutions was enhanced upon increasing NQ concentration. The impact of 3-amino-1,2,4-triazole-5-thiol (ATAT) on the corrosion inhibition of aluminum in freely aerated stagnant 3.5 wt % NaCl solution, using the cyclic polarization (CP) and EIS techniques, was reported.[8] The authors showed that the inhibition activity was dependent on the number of active centers in the corrosion inhibitor molecule, molecule size, and the mode of adsorption. El-Shafei et al. provided details regarding the utilization of tryptamine, tryptophan, and indole as corrosion inhibitors for an aluminum in 0.1 molar sodium chloride solution, employing the PDP technique.[9] Solmaz et al. examined the inhibition adequacy of $H_2C_2O_4$ acid as a corrosion inhibitor for aluminum in sodium chloride solution (pH 2), using the polarization of resistance (R_p), PDP, and EIS techniques.[10] Furthermore, 8-HQ,[11] sulfathiazole,[12] monoethanolamine,[13] diisopropyl thiourea,[14] calcium gluconate,[15] 3-amino-1,2,4-triazole-5-thiol,[16] 4-amino benzenesulfonamide, benzamide (BA), thioacetamide,[17] 2,6-dimethylpyridine,[18] octylphosphonic acid, and 2-mercaptobenzimidazole[19] were examined as corrosion inhibitors for aluminum in chloride media.

Microbial-induced corrosion is one of the main problems in the pulp and paper industry, marine industry, natural gas transmission, metal working, chemical process industries, and industrial water transmission. This type of corrosion is called biocorrosion. Bacterial or microbial corrosion is the deterioration of nonmetal or metal materials as a result of the metabolic activity of microorganisms.[20,21] Biocorrosion is often due to collaboration of physical, chemical, mechanical, and/or biological variables. Water, wind, dust particles, and atmospheric pollution cause damage to the materials, allowing penetration of moisture and aggregation of microbes on the surface. This permits the development of a biofilm, a biologically active layer of different kinds of microbes as well as mucus that is the result of their metabolic activity. Biofilm creates a good medium for growing microbes and increases the rate of corrosion up to 10,000 times.[22,23] The biocorrosion mechanism can be explained on the premise that the biofilm comprises bacterial cells and extracellular polymeric substances (combination of proteins, polysaccharides, fats, and nucleic acids) that facilitate the attachment of bacterial cells to the surface, enhancing the rate of corrosion. The biofilm also involves inorganic sludge from water and/or corrosion products.[24,25]

Despite the previously mentioned reports that have documented corrosion inhibitors for aluminum, the corrosion impediment ability of 3,3′-methylenedisalicylic acid (MDS) for aluminum in neutral chloride medium (3.5% NaCl) has not been accomplished until now. In fact, MDS (Figure 1) has acquired prominence due to its known biological activity[26] in addition to its expected corrosion impediment properties. The lone pairs of electrons on the heteroatoms (O) and presence of π bonds in the entire structure are suggested to be significant factors that induce the adsorption of MDS on the aluminum surface. It is noteworthy that methylenedisalicylic acid can form solid complexes with copper, silver, lead and aluminum.[27] Other than MDS being utilized as a polyfunctional

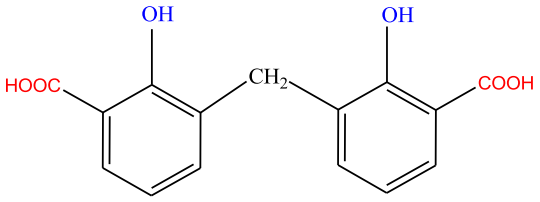

Figure 1. Structure of 3,3′-methylenedisalicylic acid.

intermediate in condensation products suitable for the surface coatings industry and plastics, it is utilized to successfully restrain the connection of ribosomes to membranes without interfering with protein synthesis.[28]

As an extension of our previous reports on the inhibitive impact of some organic compounds containing an oxygen heteroatom,[29−34] the impact of small concentrations of the isolated 3,3′-methylenedisalicylic acid on the corrosion of pure aluminum has been researched. The probable structure of the synthesized inhibitor (MDS) has been identified, and its biological action against fungi and bacteria has been examined.

2. EXPERIMENTAL SECTION

2.1. Materials and Methods. All reagents were of highest grade available from BDH and used without further purification. Microanalyses (C, H) were performed as described elsewhere.[35] The IR spectrum was recorded on Thermo Scientific iS50 Fourier transform infrared (FT-IR) spectrometer using the attenuated total reflectance technique. Electronic spectra (in ethanol) were obtained using a Shimadzu (UV-1900) spectrophotometer between 200 and 1100 nm. Mass spectrometry was performed on the direct inlet part of the mass analyzer on a Thermo Scientific GCMS model ISQ. The mass spectroscopy was performed in electron impact mode. ^{1}H NMR (400 MHz) measurement in dimethyl sulfoxide (DMSO-d_6) at room temperature (RT) was done on a Bruker spectrometer. The chemical shifts are quoted in δ (ppm) with the aid of an internal reference (tetramethylsilane, TMS).

For electrochemical measurements, a traditional three-electrode electrochemical cell that accommodates for 0.25 L of solution was used. The working electrode had a 99.999% pure aluminum electrode that was purchased from Goodfellow (located at Ermine Business Park, Huntingdon, England). The reference electrode was a silver−silver chloride (Ag/AgCl in saturated KCl solution), and the counter electrode was a Pt sheet. Electrochemical experiments were performed using a PGSTAT-302N Autolab potentiostat−galvanostat. The potentiodynamic cyclic polarization (PCP) data were obtained between −1.8 and −0.5 V at a scan rate of 0.00166 V/s. EIS plots were collected from the values of the corrosion potential for a frequency scan range between 100000 and 0.1 Hz. The chronoamperometric current−time (CCT) curves were acquired at −0.6 V. For the surface morphology of the tested Al surfaces after the electrochemical tests were performed, scanning electron microscopy (SEM) (model JSM-7400F) and an energy-dispersive X-ray (EDX) analyzer were employed. Those SEM and EDX instruments were purchased from JEOL (Tokyo, Japan).

2.2. Preparation of the Inhibitor (MDS). 3,3′-Methylenedisalicylic acid, the structural formula shown in Figure 1, was prepared using the procedure described in the literature[36,37] as follows: 9.4 g of 30% formaldehyde, 27.6 g

https://doi.org/10.1021/acsomega.2c00194
ACS Omega 2022, 7, 19193−19203

salicylic acid, and 180 g of 50% sulfuric acid were refluxed for 8 h. The powder obtained was cooled, filtered off, and washed thoroughly with cold water as well as a hot water/ethanol solution to eliminate excess unreacted salicylic acid. The separated cream powder was recrystallized from acetone and finally dried in air for 48 h [exp/lit. mp = 238 °C (decompose)].

2.3. Screening of Antimicrobial Activity of MDS. The synthesized inhibitor was screened for antimicrobial activity against six different test organisms including (i) fungi (*Aspergillus famigatus* RCMB 002008 and *Candida albicans* RCMB 005003(1) ATCC 10231) using ketoconazol as reference, (ii) Gram-positive bacteria (*Staphylococcus aureus* ATCC 25923 and *Bacillus subtilis* RCMB 0153(1) NRRL B-543) with gentamycin, and (iii) Gram-negative bacteria (*Escherichia coli* ATCC 25922 and *Proteus vulgaris* 004(1) ATCC 13315) using also gentamycin as reference. The susceptibility tests were performed by the NCCLS proposals (National Committee for Clinical Lab Standards, 1993). Assessments with respect to the restraint zone were done by the diffusion agar technique.[38,39] The inoculum suspension was synthesized from colonies grown overnight on an agar plate and inoculated into Mueller−Hinton broth. A sterile swab was immersed in the suspension and used to inoculate Mueller−Hinton agar plates. The sample was tested in DMSO at a concentration of 20 mg/mL. The inhibition zone was measured at 37 °C at the end of incubation period (i.e., 24 h). Controls utilizing DMSO were satisfactorily done.

3. RESULTS AND DISCUSSION

3.1. Chemistry and Characterization of MDS. 3,3′-Methylenedisalicylic acid was isolated in a pure form, and its analytical and physical data are depicted in Table 1. The MDS was found to be freely soluble in acetone, alcohol, normal ether, carbon tetrachloride, dimethyl sulfoxide, and dimethylformamide.

The structural formula of the synthesized MDS inhibitor (Figure 1) was validated on the premise of elemental analyses (C, H) and spectral (IR, mass, ^{1}H NMR and UV−vis) measurements.

3.1.1. IR Spectrum. The most important IR assignments for MDS are displayed in Table 1 and Figure 2. The spectrum appeared for $\nu(OH)_{phenolic}$, $\delta(OH)_{phenolic}$, $\nu(C-O)_{phenolic}$, and $\nu(C{=}O)_{carboxylic}$ at 3430, 1290, 1218, and 1658 cm^{-1}, respectively. The $\nu(C{=}O)$ absorption for the COOH group is decreased due to the internal conjugation (lone pair on oxygen in conjugation with C=O) and the presence of MDS as a dimer owing to the intermolecular hydrogen bonding between COOH groups (structure I). Establishment of a −C=O···H−O−C bridge diminished the force constants, and thus, $\nu(C{=}O)_{carboxylic}$ and $\nu(OH)_{carboxylic}$ absorptions occurred at lower wavenumbers.

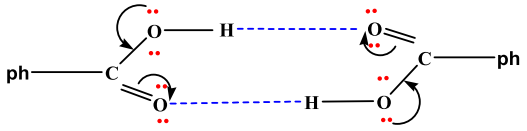

On the other hand, observation of phenolic OH at a lower position (3220 cm^{-1}) is taken as proof of the persistence of intermolecular H-bonding (O−H···O−H) between associated molecules in the solid state. The recommendation of an intermolecular H-bond between phenolic −OH comes from the broadening shape of $\nu OH_{phenolic}$, whereas bands arising

Table 1. Analytical, Physical, and Significant IR Data of 3,3′-Methylenedisalicylic Acid

compound (formula/symbol)	color	melting point	yield (%)	found (calcd) %		IR data, wavenumber (cm^{-1})				
				C	H	$\nu(OH)_{phenolic}$	$\delta(OH)_{phenolic}$	$\delta(C-O)_{phenolic}$	$\nu(OH)_{carboxylic}$	$\nu(C{=}O)_{carboxylic}$
3,3′-methylenedisalicylic acid ($C_{15}H_{12}O_6$/DMS)	cream	238 °C (decompose)	96	61.08 (62.50)	5.10 (4.20)	≈3220	1287	1203	2400−3400	1652

https://doi.org/10.1021/acsomega.2c00194
ACS Omega 2022, 7, 19193−19203

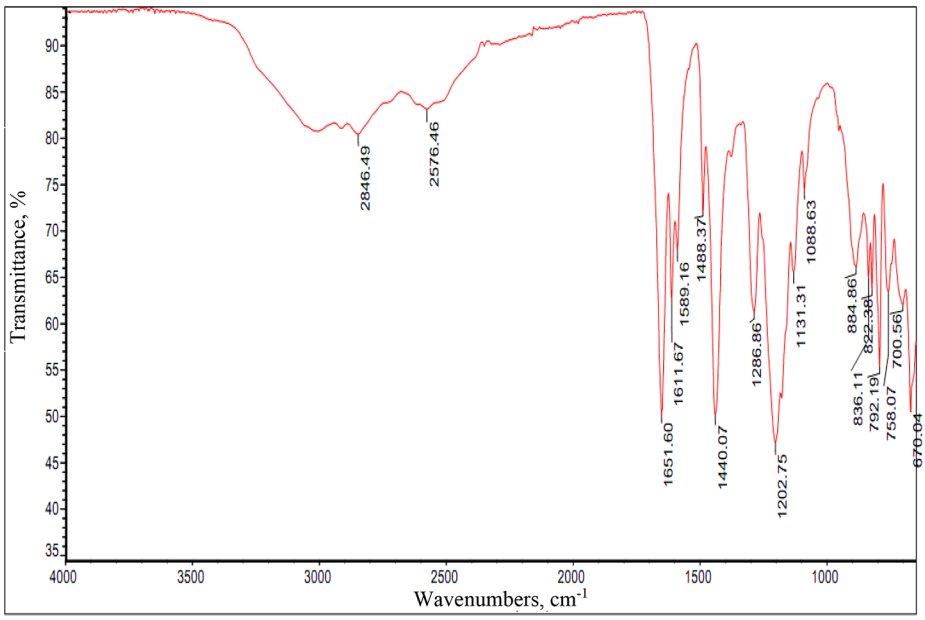

Figure 2. FT-IR spectrum of MDS.

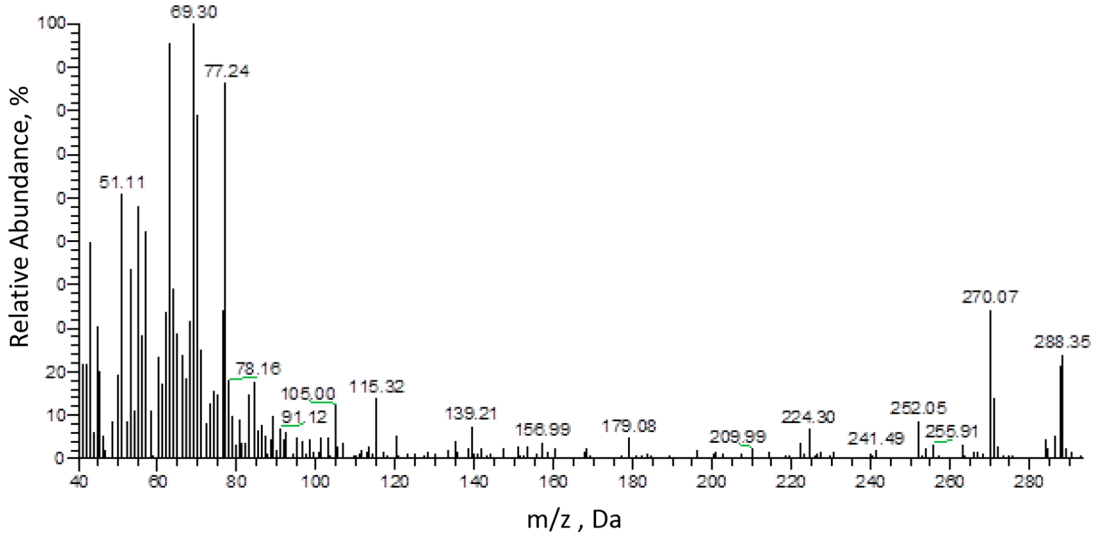

Figure 3. Mass spectrum of MDS.

from intramolecular hydrogen bonds are sharp. The remarkable downward frequency shift signifies the strength of this bond. MDS also revealed four bands situated at 1440, 1488, 1589, and 1612 cm^{-1} related to $\nu(C{=}C)_{aromatic}$. Additionally, MDS exhibited a strong band at 792 cm^{-1} assignable to the out-of-plane deformation of the aromatic rings. The positions of other bands assigned to the $\nu CH_{aromatic}$ (near 3030 cm^{-1}) and methylene ($-CH_2-$) groups (νCH_{asym} = 2910, νCH_{sym} = 2846, and $\delta CH_{rocking}$ = 758 cm^{-1}) are seen in the spectrum (Figure 1).

3.1.2. Mass Spectrum. The mass spectrum of MDS (Figure 3) emphasized the purity of the compound as well as the expected molecular weight. The MDS inhibitor provided a molecular ion peak at m/z = 288.35 [24%, ($C_{15}H_{12}O_6$), calcd m/z = 288.35].

3.1.3. NMR Spectrum. The ^1H NMR spectrum of MDS (Figure 4) uncovered signals at 11.6 (phenolic OH, s, broad), 11.2 (COOH, s, broad), 3.8 (CH_2, d), and 6.7−7.9 (aromatic protons, m). Vanishing signals of −COOH and −OH upon D_2O addition indicated the right locations of these groups where the protons in −COOH and −OH− groups are labile (acidic protons) and can be easily exchanged by deuterium, resulting in the disappearance of labile proton peaks. The broadening of $OH_{phenolic}$ and COOH signals in the spectrum provided evidence for the establishment of intermolecular hydrogen bonding for these groups, consistent with the IR results. The signal at 4.4 ppm (Figure 4b) arises from excess D_2O which was added to follow the hydroxyl and carboxylic protons in the MDS structure.

3.1.4. Electronic Spectrum. The UV−vis spectrum of the inhibitor (MDS) (Figure 5) was scanned in ethanol and gave a remarkable broad peak between 285 and 350 nm, which was assigned to overlapped $n{\rightarrow}\pi^*$ $(C{=}O)_{COOH}$ and $n{\rightarrow}\pi^*$ $(OH)_{COOH}$. The later transition was assumed considering that there was an internal conjugation in the carboxylic group (structure I). The three bands at 281, 279, and 277 nm are

https://doi.org/10.1021/acsomega.2c00194
ACS Omega 2022, 7, 19193−19203

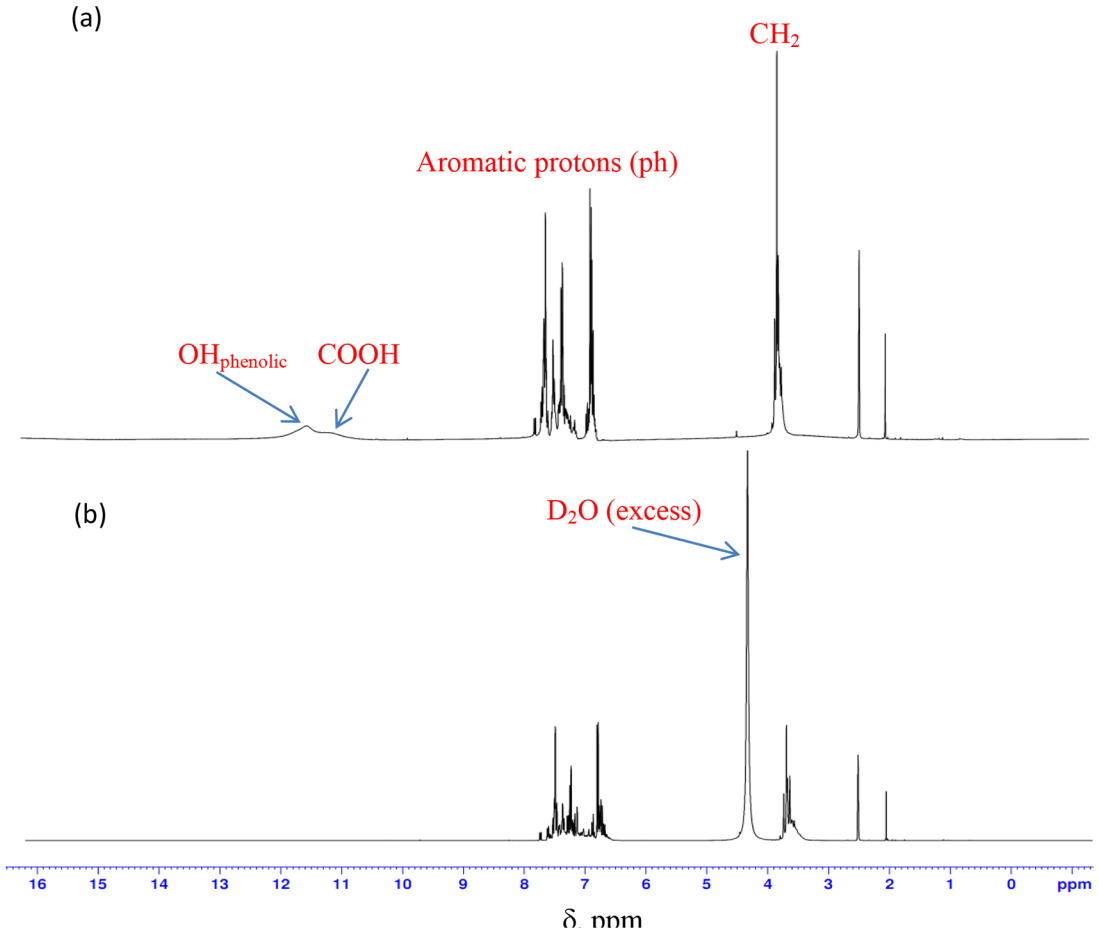

Figure 4. ^{1}H NMR spectrum of the MDS in (a) DMSO-d_6 and (b) DMSO-d_6 + D_2O.

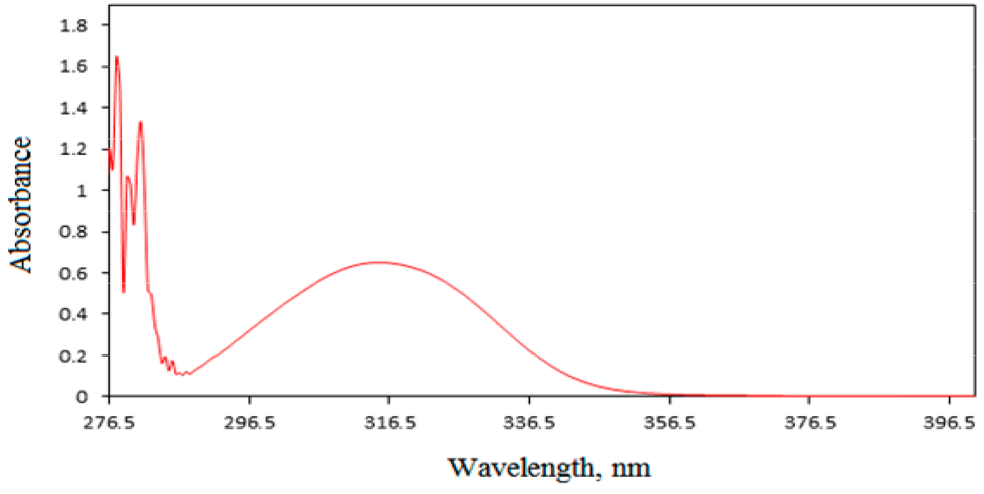

Figure 5. Electronic spectrum of MDS.

most likely due to $\pi \rightarrow \pi^*$ (C═O), $\pi \rightarrow \pi^*$ $(OH)_{COOH}$, and $\pi \rightarrow \pi^*$ (phenyl) transitions, respectively.

3.2. Antibacterial Investigation. In view of the information provided above, antimicrobial evaluation of MDS was performed. Screening of antimicrobial activity of a synthesized inhibitor revealed that the MDS inhibitor exhibits moderate activity against the test organisms including fungi as well as Gram-positive and Gram-negative bacteria (Figure 6). Although the inhibitor did not show higher activity in comparison to the standard, it has effective action toward the tested strains of both fungi and bacteria, and this may be considered a characteristic property. Figure 6 shows that MDS has a good action against fungi, especially *Candida albicans*. Note that benzoic and salicylic acids used in combination also inhibit fungal growth. Whitfield's ointment contains benzoic and salicylic acid in a 2:1 ratio that is used to prevent fungal growth.[40] The antimicrobial impact of MDS can be illustrated on the basis where MDS penetrates into lipid membranes and

https://doi.org/10.1021/acsomega.2c00194
ACS Omega 2022, 7, 19193−19203

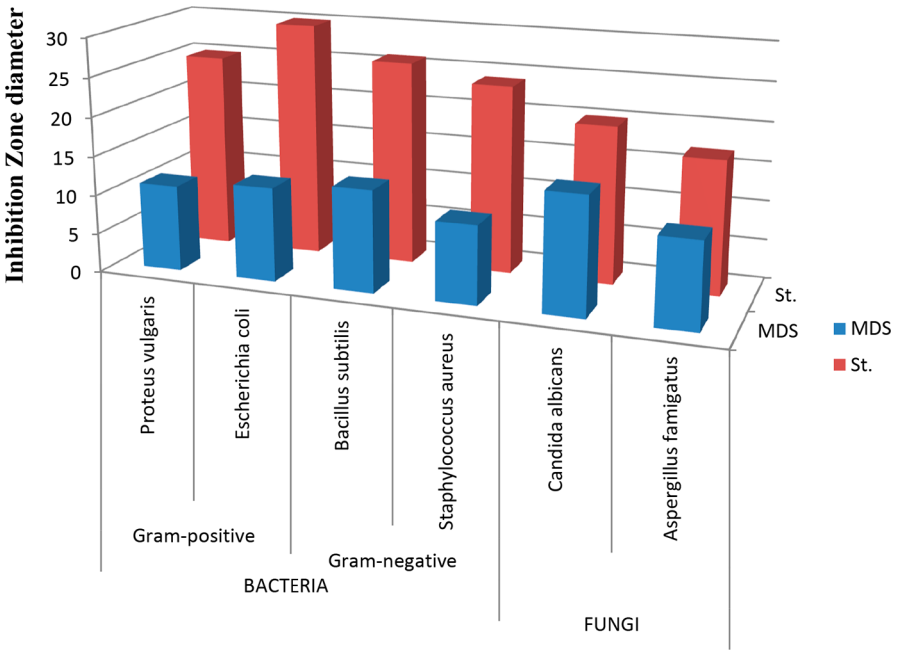

Figure 6. Antimicrobial activity for the MDS inhibitor.

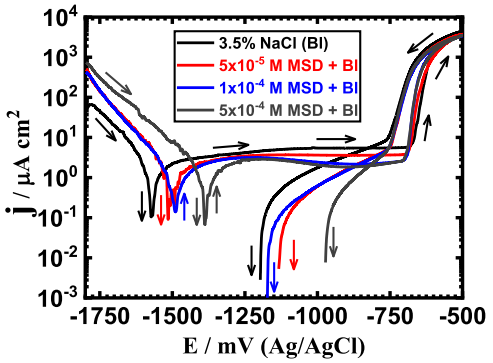

Figure 7. PCP curves for Al after 1 h immersion in 3.5% NaCl solutions in the absence and presence of MDS concentrations.

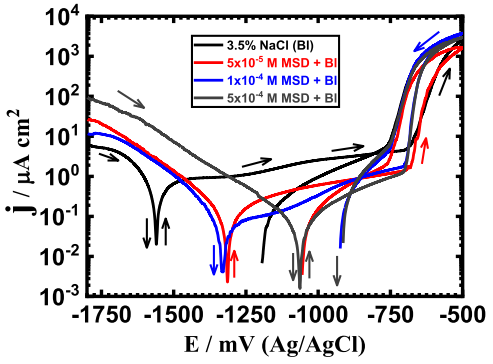

Figure 8. PCP curves for Al after 24 h immersion in 3.5% NaCl solutions in the absence and presence of MDS concentrations.

blocks of the metal binding sites in the enzymes of microorganisms.[38,41] This behavior led to the destruction of the enzymes and hence impeded the formation of proteins necessary for further growth of the organisms.[42]

3.3. Corrosion Measurements. *3.3.1. Potentiodynamic Cyclic Polarization.* The PCP curves obtained for Al after 1 h immersion in 3.5% NaCl solutions in the absence and presence of MDS concentrations are depicted in Figure 7. In order to investigate the influence of prolonging the immersion time on the corrosion and corrosion inhibition of Al in the chloride solution in the absence and presence of MDS, the PCP measurements were obtained also after 24 h, and the curves are displayed in Figure 8. The values of the corrosion characteristics that were obtained from the polarization data are summarized in Table 2. The symbols of these corrosion data can be defined as follows: β_c and β_a are the cathodic and anodic Tafel slopes, respectively; E_{Corr} and j_{Corr} are the corrosion potential and corrosion current density, respectively; R_{Corr} is the corrosion current, and R_p is the polarization resistance. The values of these corrosion parameters were obtained as reported in previous work.[32,33,43,44]

It is clear from Figure 7 that the obtained currents in the cathodic branch decrease, whether MDS is absent or present within the chloride solutions. The cathodic reaction was reported at this condition to be the reduction of oxygen as follows:[44]

$$2H_2O + O_2 + 4e^- = 4OH^- \quad (1)$$

The current increases again in the anodic side based on the application of less negative potential values. Al here shows an active passive behavior, where the increase of the currents with potential slows, allowing the curves to show a wide passive region. Such a region is composed as a result of Al oxide (Al_2O_3) formation as per the following reactions:[44]

$$Al + 3OH^- = Al(OH^-)_3 + 3e^- \quad (2)$$

This film is adsorbed on the surface of Al and transfers into Al_2O_3 as follows:

$$Al(OH^-)_3 = Al_2O_3 \cdot 3H_2O \quad (3)$$

The adsorption of this $Al_2O_3 \cdot 3H_2O$ onto the surface of Al is responsible for the partial protection of the surface as well as the appearance of the long passive region. Further increasing of the applied potential leads to an abrupt increase in the current

https://doi.org/10.1021/acsomega.2c00194
ACS Omega 2022, 7, 19193−19203

Table 2. Corrosion Parameters Obtained from the Potentiodynamic Cyclic Polarization Curves

solution	β_c (mV/dec)	E_{Corr} (mV)	β_a (mV/dec)	j_{Corr} (μA/cm^2)	R_P (kΩ cm^2)	R_{Corr} (mm y^{-1})
3.5% NaCl alone (1 h)	75	−1570	150	1.0	21.74	0.01091
3.5% NaCl + 5 × 10^{-5} M MDS (1 h)	72	−1505	130	0.82	24.57	0.00894
3.5% NaCl + 1 × 10^{-4} M MDS (1 h)	68	−1490	115	0.65	28.58	0.00709
3.5% NaCl + 5 × 10^{-4} M MDS (1 h)	65	−1395	105	0.50	34.91	0.00545
3.5% NaCl alone (24 h)	110	−1545	140	0.85	31.51	0.00927
3.5% NaCl + 5 × 10^{-5} M MDS (24 h)	100	−1310	130	0.17	144.6	0.00185
3.5% NaCl + 1 × 10^{-4} M MDS (24 h)	93	−1310	115	0.06	372.6	0.00065
3.5% NaCl + 5 × 10^{-4} M MDS (24 h)	85	−1060	100	0.03	665.9	0.00033

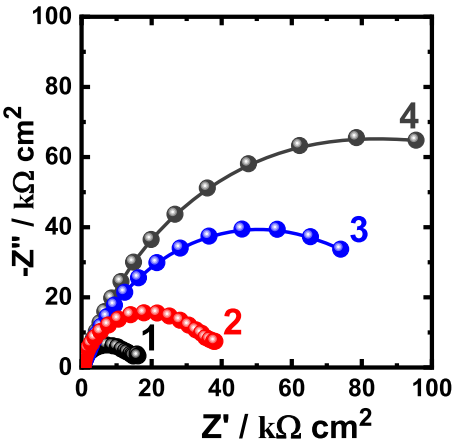

Figure 9. Nyquist plots for Al after 1 h immersion in (1) 3.5% NaCl solutions in the absence and presence of (2) 5 × 10^{-5} M MDS, (3) 1 × 10^{-4} M MDS, and (4) 5 × 10^{-4} M MDS.

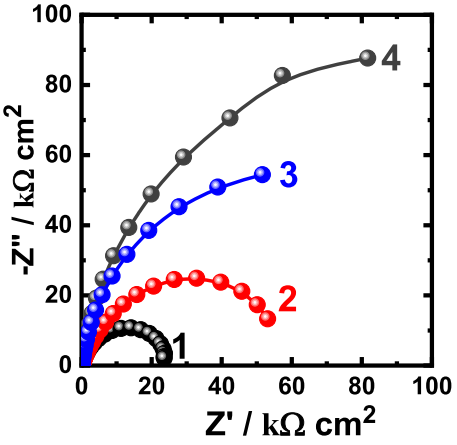

Figure 10. Nyquist plots for Al after 24 h immersion in (1) 3.5% NaCl solutions in the absence and presence of (2) 5 × 10^{-5} M MDS, (3) 1 × 10^{-4} M MDS, and (4) 5 × 10^{-4} M MDS.

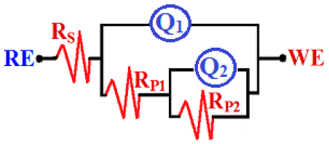

Figure 11. Equivalent circuit represents the best EIS data fit.

values as a result of the breakdown of the formed Al_2O_3 film and the occurrence of pitting corrosion. This was further indicated by reversing the applied potential to be scanned in the backward direction and leads to the appearance of a hysteresis loop (HL), which is due to the higher current values in the reverse direction as compared to the current values obtained from the forward scan direction.

The presence of 5 × 10^{-5} M MDS is seen to highly reduce the uniform corrosion of Al via decreasing the recorded currents in the cathodic and anodic branches. This effect reflects the decrease of the value of j_{Corr} and thus reduces the value of R_{Corr} and increases the value of R_P. Increasing the concentration of MDS to 1 × 10^{-4} M and further to 5 × 10^{-4} M further decreases the values of j_{Corr} and R_{Corr} with increasing values of R_P. This results from the adsorption of MDS molecules on the surface of Al, which results in the reduction of the severity of NaCl. The effect of MDS molecules not only limits the inhibition of the uniform corrosion of Al but also minimizes the severity of the pitting attack via reducing the size of HL. The increase of the concentration of MDS leads to the reduction of the size of HL due to the lower current values. This effect was supported by the data recorded for Al after 1 h immersion in the different test solutions and is listed in Table 2, where the values of j_{Corr} and R_{Corr} decrease, while R_P values increase with the increase of MDS content.

Increasing the immersion time to 24 h (Figure 8) before measurement was also found to decrease the corrosion of Al in the chloride solution. This was proven by the decrease of the cathodic and anodic currents, the current values in the passive region, the values of j_{Corr} and R_{Corr}, and the increase of R_P. This is due to the thickening of the formed oxide film onto the surface of Al as a result of the long exposure time. The addition of 5 × 10^{-5} M MDS and the increase of this concentration to 1 × 10^{-4} M MDS and further to 5 × 10^{-4} M MDS with the chloride solution for 24 h were also found to remarkably inhibit the corrosion of Al compared to its intensity after only 1 h immersion (Figure 7). This was confirmed by the decrease of currents as shown in Figure 8 and also the values of the corrosion parameters that are listed in Table 2. The polarization measurements thus indicated that the corrosion of Al decreases in the presence of MDS and with the increase of its concentration, and this effect also increases with prolonged immersion time from 1 to 24 h.

3.3.2. Electrochemical Impedance Spectroscopy. In order to confirm the obtained polarization data in studying the inhibition of Al corrosion in the chloride solution by MDS molecules, EIS experiments were performed at the same condition. Figure 9 displays the Nyquist plots that were collected for Al after 1 h immersion in (1) 3.5% NaCl solutions in the absence and presence of (2) 5 × 10^{-5} M MDS, (3) 1 × 10^{-4} M MDS, and (4) 5 × 10^{-4} M MDS. The Nyquist plots were also obtained for Al after 24 h immersion at the same conditions, and the spectra are seen in Figure 10. These EIS data were fitted using ZSimpWin v.3 software program, and the best equivalent circuit is depicted in Figure 11. This circuit has been employed as the best fit in many other studies.[43,45] The

https://doi.org/10.1021/acsomega.2c00194
ACS Omega 2022, 7, 19193−19203

Table 3. EIS Tabulated Values for Al in Chloride Solutions with and without MDS Present

		Q_1			Q_2		
solution	R_s (Ω cm^2)	Y_{Q_1} (F cm^{-2})	n	R_{P1} (kΩ cm^2)	Y_{Q_2} (F cm^{-2})	n	R_{P2} (kΩ cm^2)
3.5% NaCl (1 h)	42.97	0.8063	0.91	1481	0.4241	0.99	8043
3.5% NaCl + 5 × 10^{-5} M MDS (1 h)	45.64	0.3107	1.0	2364	0.3323	0.91	10776
3.5% NaCl + 1 × 10^{-4} M MDS (1 h)	48.32	0.1154	1.0	4913	0.2099	0.74	13210
3.5% NaCl + 5 × 10^{-4} M MDS (1 h)	51.81	0.0693	0.92	5179	0.1361	0.90	18615
3.5% NaCl (24 h)	47.69	0.6181	1.0	5085	0.0980	0.79	10830
3.5% NaCl + 5 × 10^{-5} M MDS (24 h)	51.37	0.2595	0.97	7518	0.0463	0.86	13000
3.5% NaCl + 1 × 10^{-4} M MDS (24 h)	56.78	0.0842	0.95	14467	0.0154	0.92	14390
3.5% NaCl + 5 × 10^{-4} M MDS (24 h)	59.13	0.0255	0.95	20334	0.0102	0.91	28385

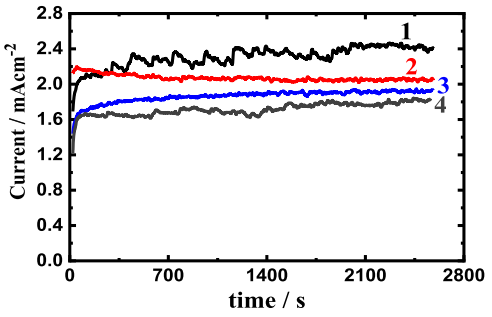

Figure 12. Chronoamperometric current−time curves collected at −600 mV (Ag/AgCl) for Al after 1 h immersion in (1) 3.5% NaCl solutions in the absence and presence of (2) 5 × 10^{-5} M MDS, (3) 1 × 10^{-4} M MDS, and (4) 5 × 10^{-4} M MDS.

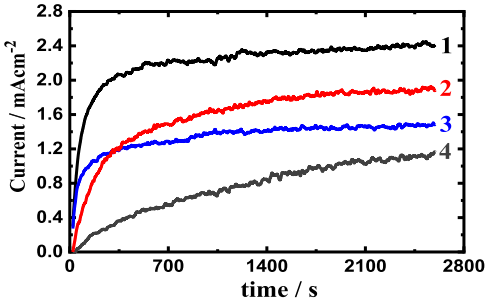

Figure 13. CCT curves collected at −600 mV (Ag/AgCl) for Al after 24 h immersion in (1) 3.5% NaCl solutions in the absence and presence of (2) 5 × 10^{-5} M MDS, (3) 1 × 10^{-4} M MDS, and (4) 5 × 10^{-4} M MDS.

parameters of the circuit can be expressed as follows: the solution resistance, R_s; the two polarization resistances, R_{P1} and R_{P2}; and two constant phase elements, Q_1 and Q_2. The values of these elements after the different immersion periods of time are gathered in Table 3. R_{P1} can be considered as the charge transfer resistance at the interface between Al and the formed oxide film, whereas R_{P2} represents the resistance at the interface between the oxide layer and the solution. Also, Q_1 and Q_2 have been previously said to estimate the deviations from the ideality.[46] Here, the presence of Q has indicated that the formed film on the surface of Al has a complex structure of two different layers and also confirmed the presence of two polarization resistances, R_{P1} and R_{P2}. Moreover, the values of n that accompany both Q_1 and Q_2 represent double-layer capacitors (C_{dl}). Thus, the outer formed layer on the surface of Al must have some pores, and therefore, the presence of MDS inhibits the corrosion of Al in this condition. The decrease of the values of Y_{Q_1} and Y_{Q_2} in the presence of MDS and further with the increase of its content gives another proof that the surface of Al is more passivated.

3.3.3. Chronoamperometric Current−Time. The CCT technique has been successfully used in the investigation of the corrosion and corrosion inhibition of metals in the 3.5% NaCl solution.[32,33,43−45] The CCT curves collected at −600 mV (Ag/AgCl) for Al after 1 h immersion in (1) 3.5% NaCl solutions in the absence and presence of (2) 5 × 10^{-5} M MDS, (3) 1 × 10^{-4} M MDS, and (4) 5 × 10^{-4} M MDS are shown in Figure 12. The currents are seen to increase in the first few moments upon the application of the constant potential value. This increase of current is due to the dissolution of the oxide film that was formed on the surface of Al during its immersion before the potential application. The current then slightly increases with time until the end of the experiment. This

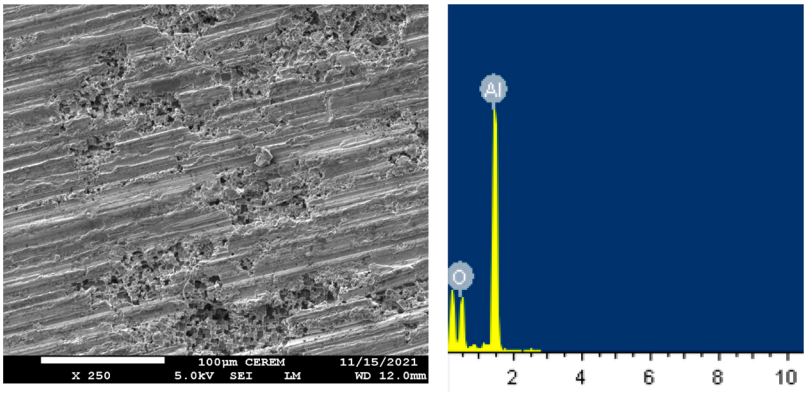

Figure 14. SEM and EDX analysis taken for the surface of Al at −600 mV after its immersion in 3.5% NaCl solution for 24 h.

https://doi.org/10.1021/acsomega.2c00194
ACS Omega 2022, 7, 19193−19203

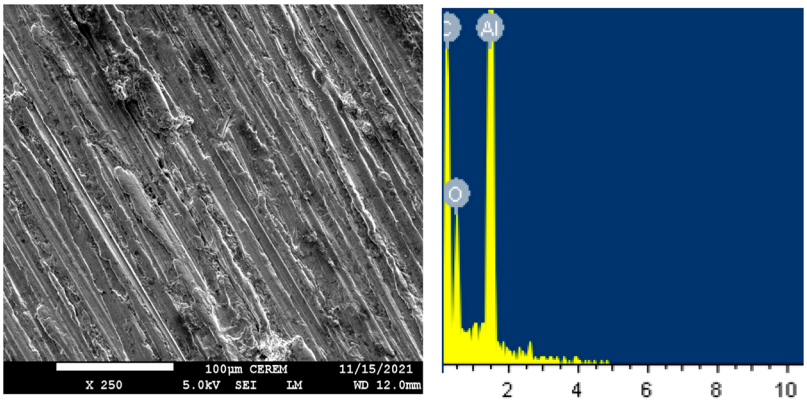

Figure 15. SEM and EDX analysis taken for the surface of Al at −600 mV after its immersion in 3.5% NaCl + 5 × 10^{-4} M MDS solution for 24 h.

behavior comes from both decreasing of the chemical inertness of the natural Al_2O_3 film and the dissolution of Al, which finally leads to the occurrence of pitting corrosion. Here, the chloride ions get adsorbed onto the surface of Al and form an oxychloride complex, $Al(OH)_2Cl_2^-$ as follows:[47−49]

$$Al^{3+} + 2Cl^- + 2OH^- = Al(OH)_2Cl_2^- \quad (4)$$

The dissolution of the aluminum may also occur as per the following reaction:

$$Al = Al^{3+} + 3e^- \quad (5)$$

The presence of Cl^- in the solution at this high anodic potential, −600 mV, allows the formation of Al chloride complex according to the reaction:[50]

$$Al^{3+} + 4Cl^- = AlCl_4^- \quad (6)$$

These surface-formed components, $Al(OH)_2Cl_2^-$ and $AlCl_4^-$, are unstable and transfer to the solution, leaving the surface causing its pitting corrosion.

The addition of 5 × 10^{-5} M MDS (Figure 12) is seen to decrease the absolute currents as well as eliminate the current fluctuations recorded for Al in NaCl solution alone. Increasing the concentration of MDS to 1 × 10^{-4} M and further to 5 × 10^{-4} M allowed Al to record less absolute currents. This means that the presence of MDS and the increase of its content in the solution decreases the uniform corrosion of Al via decreasing its current with time. Also, the disappearance of current fluctuations indicates that MDS reduces the occurrence of pitting corrosion.

The CCT curves obtained after increasing the immersion time to 24 h before measurements (Figure 13) showed that the initial currents are very low compared to the ones obtained after only 1 h at the same condition. This is because of the thick oxide film formed during the immersion of Al for 24 h and indicates that the long immersion time increases the resistance to corrosion at −600 mV. The currents abruptly increase with increasing time of the applied potential due to the dissolution of the formed oxide film. The presence of MDS is seen to greatly decrease the absolute values of the current, and this effect increases with the increase of the MDS concentration. The CCT data thus agree with the results obtained from PCP and EIS measurements.

3.3.4. Surface Examination. Figure 14 displays the SEM graph and the EDX analysis of the Al electrode that was kept on hold for 1 h at a potential of −600 mV after being immersed in 3.5% NaCl solution for 24 h. The SEM image shows many pits on the surface of Al due to the attack of the surface by the chloride solution at this anodic potential, −600 mV. The EDX profile shown in the figure indicates that there is only Al and O. The weight percentage of Al was recorded to be 82.72%, whereas for O, it was only 17.28%. The percentages of the detected Al and O indicate that the surface is partially covered with aluminum oxide, which results from the reaction of the Al surface and the O that is present in the solution. On the other hand, the majority of the Al electrode's surface is full of pits, which have no oxides inside it. This also confirms that NaCl solution has a harsh impact on Al in this condition.

In order to see the surface morphology and the compounds which may be formed on the surface of the Al electrode after its immersion in the chloride solution containing MDS molecules, SEM and EDX investigations were performed. The SEM micrograph and EDX spectrum collected from the surface of Al in 3.5% NaCl + 5 × 10^{-4} M MDS solution at −600 mV are shown in Figure 15. It is seen from the SEM image that the surface has a thick corrosion product layer with only a few pits. Compared to the SEM image for Al in NaCl without MDS present (Figure 14), the surface of Al in NaCl + MDS is more protected owing to the ability of MDS to inhibit Al corrosion. EDX analysis of the Al surface at this condition recorded only 64.46% Al, 27.72% C, and 7.82% O. This indicates that the surface has MDS molecules adsorbed, in addition to the presence of a lower percentage of aluminum oxide. The presence of the adsorbed MDS molecules thus leads to the protection of the surface via reducing the intensity of the pitting corrosion. The SEM and EDX investigations thus confirm the electrochemical behavior that Al suffers both uniform and pitting corrosion in NaCl solution, and the presence of MDS molecules reduces the attack of the chloride ions, which in turn protects Al against corrosion.

4. CONCLUSIONS

3,3′-Methylenedisalicylic acid can be prepared from salicylic acid, formaldehyde, and sulfuric acid. Elemental analysis (C and H), FT-IR, mass, NMR, and UV−vis spectroscopy are powerful techniques to recognize the identity of the MDS compound. The corrosion inhibition efficiency of MDS molecules at different concentrations was tested on Al corrosion in 3.5% NaCl solution using different electrochemical and spectroscopic measuring techniques. PCP results indicated that the presence of MDS and the increase of its concentration significantly inhibit the corrosion of Al via reducing its corrosion rate. The impedance, EIS, experiments

https://doi.org/10.1021/acsomega.2c00194
ACS Omega 2022, 7, 19193−19203

revealed that MDS greatly increases the polarization resistance of Al, and this effect increases with the increase of MDS concentration as well as the increase of immersion time from 1 to 24 h. CCT curves taken for Al after 24 h immersion and at −600 mV also confirmed that the presence of MDS and the increase of its concentration led to the uniform attack of Al and remarkably reduced its pitting corrosion. The SEM and EDX analyses confirmed the electrochemical measurements that showed the corrosion of Al in NaCl solution is greatly inhibited upon the addition of MDS and with the increase of its content in the solution. Probably the hypothesis of hard and soft acids and bases (HSAB) can likewise clarify the theory of inhibition. As indicated by Pearson's guideline,[51,52] metals are classified into three classes, namely, hard acids, soft acids, and intermediate acids. Bases are likewise classified into hard, soft, and intermediate bases. Hard metals, having charge/size equally high, tend to bind with hard bases containing O: and F^- donor atoms. Based on this supposition alongside the obtained data, it can be concluded that aluminum ions (Al^{3+}), which represent hard acids, will bind strongly with the inhibitor-containing O donor atoms in its structure (Figure 1). The investigated inhibitor was assayed for its antimicrobial activity toward some types of bacteria and fungi. The results suggested that the MDS might inhibit the growth of some microbes.

AUTHOR INFORMATION

Corresponding Author

Ayman H. Ahmed − *Chemistry Department, College of Science and Arts, Jouf University, Gurayat 2014, Saudi Arabia;* orcid.org/0000-0001-6180-8562; Email: ahfahmi@ju.edu.sa

Author

El-Sayed M. Sherif − *Center of Excellence for Research in Engineering Materials (CEREM), College of Engineering, King Saud University, Al-Riyadh 11421, Saudi Arabia*

Complete contact information is available at: https://pubs.acs.org/10.1021/acsomega.2c00194

Notes

The authors declare no competing financial interest.

ACKNOWLEDGMENTS

The authors extend their appreciation to the Deanship of Scientific Research at Jouf University for funding this work through research grant (No. DSR-2021-03-0220).

REFERENCES

(1) Davis, J. R. *Corrosion of Aluminum and Aluminum Alloys*; ASM International, 1999.

(2) Xhanari, K.; Finsgar, M. Organic corrosion inhibitors for aluminum and its alloys in acid solutions: a review. *RSC Adv.* **2016**, *6*, 62833−62857.

(3) Xhanari, K.; Finsgar, M. Organic corrosion inhibitors for aluminum and its alloys in chloride and alkaline solutions: A review. *Arab. J. Chem.* **2019**, *12*, 4646−4663.

(4) Lopez-Sesenes, R.; Gonzalez-Rodriguez, J. G.; Casales, M.; Martinez, L.; Sanchez-Ghenno, J. C. Corrosion Inhibition of Carbon Steel in 0.5M HCl by Monopropianate. *Int. J. Electrochem. Sci.* **2011**, *6*, 1772−1784.

(5) Matter, E. A.; Kozhukharov, S.; Machkova, M.; Kozhukharov, V. Electrochemical studies on the corrosion inhibition of AA2024 aluminum alloy by rare earth ammonium nitrates in 3.5% NaCl solutions. *Mater. Corros.* **2013**, *64*, 408−414.

(6) Rodic, P.; Milosev, I. Corrosion inhibition of pure aluminum and alloys AA2024-T3 and AA7075-T6 by Cerium(III) and cerium(IV) salts. *J. Electrochem. Soc.* **2016**, *163*, C85−C93.

(7) Sherif, E. M.; Park, S.-M. Effects of 1,5-Naphthalenediol on aluminum corrosion as a corrosion inhibitor in 0. *50 M NaCl. J. Electrochem. Soc.* **2005**, *152*, B205−B211.

(8) Sherif, E.-S. M. effects of 3-amino-1,2,4-triazole-5-thiol on the inhibition of pure aluminum corrosion in aerated stagnant 3.5 wt.% NaCl solution as a corrosion inhibitor. *Int. J. Electrochem. Sci.* **2012**, *7*, 4847−4859.

(9) El-Shafei, A.A; Abd El-Maksoud, S.A; Fouda, A.S The role of indole and its derivatives in the pitting corrosion of Al in neutral chloride solution. *Corros. Sci.* **2004**, *46*, 579−590.

(10) Solmaz, R.; Kardas, G.; Yazıcı, B.; Erbil, M. Citric acid as natural corrosion inhibitor for aluminum protection. *Corros. Eng. Sci. Technol.* **2008**, *43*, 186−191.

(11) Garrigues, L.; Pebere, N.; Dabosi, F. An investigation of the corrosion inhibition of pure aluminum in neutral and acidic chloride solutions. *Electrochim. Acta* **1996**, *41*, 1209−1215.

(12) Zor, S.; Sağdinc, S. Experimental and theoretical study of sulfathiazole as environmentally friendly inhibitor on aluminum corrosion in NaCl. *Prot. Metals Phys. Chem. Surf.* **2014**, *50*, 244−253.

(13) Jevremovic, I.; Stankovic, V. M. The Inhibitive effect of ethanolamine on corrosion behavior of aluminum in NaCl solution saturated with CO_2. *Metall. Mater. Eng.* **2012**, *18*, 241−257.

(14) Lakshmi, N. V.; Arivazhagan, N. The corrosion inhibition of aluminum in 3.5% NaCl by diisopropyl thiourea. *Int. J. Chem. Tech Res.* **2013**, *5*, 1959−1963.

(15) Hakeem, M.; Rajendran, S. Calcium gluconate as a corrosion inhibitor for aluminium. *J. Eng., Comput. Appl. Sci.* **2014**, *3*, 1−11.

(16) Sherif, E.-S. M. Electrochemical investigations on the corrosion inhibition of aluminum by 3-amino-1,2,4-triazole-5-thiol in naturally aerated stagnant seawater. *J. Ind. Eng. Chem.* **2013**, *19*, 1884−1889.

(17) Zor, S.; Ozkazanc, H. The inhibition effect of amides on aluminum corrosion in chloride solutions. *Prot. Metals Phys. Chem. Surf.* **2010**, *46*, 727−733.

(18) Padash, R.; Sajadi, G. S.; Jafari, A. H.; Jamalizadeh, E.; Rad, A. S. Corrosion control of aluminum in the solutions of NaCl, HCl and NaOH using 2,6-dimethylpyridine inhibitor: Experimental and DFT insights. *Mater. Chem. Phys.* **2020**, *244*, 122681.

(19) Kozlica, D. K.; Kokalj, A.; Milošev, I. Synergistic effect of 2-mercaptobenzimidazole and octylphosphonic acid as corrosion inhibitors for copper and aluminum − an electrochemical, XPS, FTIR and DFT study. *Corros. Sci.* **2021**, *182*, 109082.

(20) Kaczerewska, O.; Brycki, B.; Leiva-García, R.; Akid, R. Cationic gemini surfactants as corrosion inhibitors of stainless steel(AISI304) in 3M hydrochloric acid. *EUROCORR Prague* **2017**, 1−10.

(21) Qiu, L.-G.; Wu, Y.; Wang, Y.-M.; Jiang, X. Synergistic effect between cationic Gemini surfactant and chloride ion for the corrosion inhibition of steel in sulphuric acid. *Corros. Sci.* **2008**, *50*, 576−582.

(22) Wu, Z.-Y.; Fang, Z.; Qiu, L.-G.; Wu, Y.; Li, Z.-Q.; Xu, T.; Wang, W.; Jiang, X. Synergistic inhibition between the Gemini surfactant and bromide ion for steel corrosion in sulphuric acid. *J. Appl. Electrochem.* **2009**, *39*, 779−784.

(23) Zhao, J.; Duan, H.; Jiang, R. Synergistic corrosion inhibition effect of quinolone quaternary ammonium salt and Gemini surfactant in H_2S and CO_2 saturated brine solution. *Corros. Sci.* **2015**, *91*, 108−119.

(24) El-Mahdy, G. A.; Atta, A. M.; Al-Lohedan, H. A.; Ezzat, A. O. Influence of green corrosion inhibitor based on chitosan ionic liquid on the steel corrodibility in chloride solution. *Int. J. Electrochem. Sci.* **2015**, *10*, 5812−5826.

(25) Muyzer, G.; Stams, A. J. M. *Nature Reviews. Microbiology* **2008**, *6*, 441.

(26) Cushman, M.; Kanamathareddy, S. Synthesis of the covalent hydrate of the incorrectly assumed structure of aurintricarboxylic acid (ATA). *Tetrahedron* **1990**, *46*, 1491−1498 and references therein.

(27) Nădăban, A.; Vlase, G. The synthesis and study of some complexes of methylenedisalicylic acid. *New Front. Chem.* **2015**, *24*, 55−60.
(28) Aporti, G.; schiatti, A.; Macconi, D.; Borgese, N. The inhibitory effect of methylenedisalicylic acid on the attachment of ribosomes to microsomal membranes in vitro. *FEBS LETTERS* **1980**, *116*, 95−98.
(29) Ahmed, A. H.; Hassan, A. M.; Gumaa, H. A.; Mohamed, B. H.; Eraky, A. M.; Omran, A. A. Copper(II)-oxaloyldihydrazone complexes: Physico-chemical studies; energy band gap and inhibition evaluation of free oxaloyldihydrazones toward the corrosion of copper metal in acidic medium. *Arab. J. Chem.* **2019**, *12*, 4287−4302.
(30) Ahmed, A. H.; Hassan, A. M.; Gumaa, H. A.; Mohamed, B. H.; Eraky, A. M. Physicochemical studies on some selected oxaloyldihydrazones and their novel palladium(II) complexes along with using oxaloyldihydrazones as corrosion resistants. *Inorg. Nano-Met. Chem.* **2017**, *47*, 1652−1663.
(31) Ahmed, A. H.; Hassan, A. M.; Gumaa, H. A.; Mohamed, B. H.; Eraky, A. M. Mn^{2+}-complexes of N,O-dihydrazone: Structural studies, indirect band gap energy and corrosion inhibition on aluminum in acidic medium. *J. Chil. Chem. Soc.* **2018**, *63*, 4180−4189.
(32) Ahmed, A. H.; Sherif, E.-S. M.; Abdo, H. S.; Gad, E. S. Ethanedihydrazide as a Corrosion Inhibitor for Iron in 3.5% NaCl Solutions. *ACS Omega* **2021**, *6*, 14525−14532.
(33) Sherif, E.-S. M.; Ahmed, A. H.; Abdo, H. S.; DefAllah, M. N. Impediment of iron corrosion by N,N'-bis[2-hydroxynaphthylidene]-amino]oxamide in 3.5% NaCl solution. *Crystals* **2021**, *11*, 1263.
(34) Sherif, E.-S. M.; Ahmed, A. H. Synthesizing new hydrazone derivatives and studying their effects on the inhibition of copper corrosion in sodium chloride solutions. *Synth. React. Inorg., Met.-Org., Nano-Met. Chem.* **2010**, *40*, 365−372.
(35) Thabet, M. S.; Ahmed, A. H. Ship-in-a-bottle synthesis and physicochemical studies on zeolite encapsulated Mn(II), Mn(III)-semicarbazone complexes: Application in the heterogeneous hydroxylation of benzene. *J. Porous Mater.* **2013**, *20*, 319−330.
(36) Clemmensen, E.; Heitman, A. H. C. Methylenedisalicylic acid and its reaction with bromine and iodine. *J. Am. Chem. Soc.* **1911**, *33*, 733−745.
(37) Sivapullaiah, P. V.; Soundararajan, S. Methylene di salicylates of rare-earths. *J. I. I. Sc.* **1976**, *58*, 289−293.
(38) Ahmed, A. H. N,N'-bis[2-hydroxynaphthylidene]/[2-methoxybenzylidene]amino]oxamides and their divalent manganese complexes: Isolation, spectral characterization, morphology, antibacterial and cytotoxicity against leukemia cells. *Open Chem.* **2020**, *18*, 426−437.
(39) Hindler, J. A.; Howard, B. J.; Keiser, J. F. Antimicrobial agents and susceptibility testing. In *Clinical and pathogenic microbiology*; Howard, B. J., Ed.; Mosby-Year Book Inc.: St. Louis, MO, 1994.
(40) Block, S. S. *Disinfection, Sterilization and Preservation*, 4th ed.; Malven Lioydia, 1991; Vol. *37*.
(41) Ahmed, A. H.; Hassan, A. M.; Gumaa, H. A.; Mohamed, B. H.; Eraky, A. M. Nickel(II)-oxaloyldihydrazone complexes: Characterization, indirect band gap energy and antimicrobial evaluation. *Cogent Chem.* **2016**, *2*, 1142820.
(42) Kavitha, P.; Laxma Reddy, K. *Arab. J. Chem.* **2016**, *9*, 596−605.
(43) Sherif, E.-S. M.; Ahmed, A. H. Alleviation of iron corrosion in chloride solution by n,n′-bis[2-methoxynaphthylidene]amino]-oxamide as a corrosion inhibitor. *Crystals* **2021**, *11*, 1516.
(44) Sherif, E.-S. M. Electrochemical investigations on the corrosion inhibition of aluminum by 3-amino-1,2,4-triazole-5-thiol in naturally aerated stagnant seawater. *J. Ind. Eng. Chem.* **2013**, *19*, 1884−1889.
(45) Alharbi, H. F.; Bahri, Y. A.; Sherif, E.-S. M. Influence of Zirconium on the Corrosion Passivation of Titanium in Simulated Body Fluid. *Crystals* **2021**, *11*, 1391.
(46) Diamanti, M. V.; Bolzoni, F.; Ormellese, M.; Pérez-Rosales, E. A.; Pedeferri, M. P. Characterization of titanium oxide films by potentiodynamic polarisation and electrochemical impedance spectroscopy. *Corros. Eng. Sci. Technol.* **2010**, *45*, 428−434.
(47) Szklarska-Smialowska, Z. Pitting corrosion of aluminum. *Corros. Sci.* **1999**, *41*, 1743−1767.
(48) Sato, N. The stability of localized corrosion. *Corros. Sci.* **1995**, *37*, 1947−1967.
(49) Hunkeler, F.; Frankel, G. S.; Bohni, H. Technical Note: On the Mechanism of Localized Corrosion. *Corrosion (NACE)* **1987**, *43*, 189−191.
(50) Badawy, W. A.; Al-Kharafi, F. M.; El-Azab, A. A. Electrochemical behavior and corrosion inhibition of Al, Al-6061 and Al−Cu in neutral aqueous solutions. *Corros. Sci.* **1999**, *41*, 709−727.
(51) Pearson, R. G. Hard and soft acids and bases, HSAB, part II: Underlying theories. *J. Chem. Educ.* **1968**, *45*, 643−648.
(52) Pearson, R. G. *Chemical Hardness—Applications from Molecules to Solids*; Wiley-VCH: Weinheim, Germany, 1997.

https://doi.org/10.1021/acsomega.2c00194
ACS Omega 2022, 7, 19193−19203